Thermochimca Acta, 43 (1981) 253—267
Elsevier Scientific Publishing Company, Amsterdam — Printed in Belgium

THERMOMAGNETOMETRY AND THERMAL DECOMPOSITION OF SIDERITE *

P.K. GALLAGHER and S.St J. WARNE **

Bell Laboratories, Murray Hill, NJ 07974 (U.S.A.)

(Received 22 April 1980)

ABSTRACT

Thermogravimetry, evolved gas analysis, thermomagnetometry and X-ray diffraction analysis were used to study the thermal decomposition of three siderites having markedly different purities. The decomposition proceeds to form wustite and carbon dioxide; however, some interaction between the two products occurs. In vacuum much of the wustite is retained but at atmospheric pressure in a flowing inert gas magnetite is the predominant product. In flowing oxygen the oxidation is so rapid that only hematite can be detected. Thermomagnetometry is useful to indicate the distribution of the major impurities, e.g., Mg and Mn. These impurities influence the extent of oxidation and stabilize a spinel phase, even in oxygen. The presence and composition of siderite is important in a number of industries, ranging from ceramic to coal and oil shale utilization.

INTRODUCTION

The literature describing various aspects of the thermal decomposition of siderite ($FeCO_3$) has been reviewed [1], considered in relation to other carbonate minerals [2], and their PA curves *** (curves of sample amount dependence) [3], while differential thermal analysis (DTA) curve modifications in response to progressive dilution and furnace atmosphere changes [4] and simultaneous thermal techniques have been applied to the kinetics and mechanism of its decomposition [5].

The major source of debate concerns the nature of the oxidation/reduction equilibria. Complicating this aspect is the wide variability in chemical composition exhibited by naturally occurring siderites, which is highlighted by the range of analyses published [6]. The substitution of Mg, Mn and to a lesser extent Ca, for Fe^{2+} is so common that pure or nearly pure siderite is seldom found [7]. Conversely, all three of these main impurity elements may be found substituting for Fe^{2+} in the same siderite [6]. Furthermore, apparently complete isomorphous series may be formed between siderite ($FeCO_3$) and magnesite ($MgCO_3$) and between siderite ($FeCO_3$) and rhodo-

* Presented at the 10th Annual NATAS Meeting, Boston, MA, 27th October 1980.
** Present address: Department of Geology, University of Newcastle, New South Wales 2308, Australia.
*** Proben-Abhängigkeit curves based on DTA determinations.

0040-6031/81/0000—0000/$02.50

chrosite ($MnCO_3$) [6], although whether the latter series is complete has been questioned [7]. The variations in chemical composition although complicating the interpretation of thermal analysis results, do appear to lead to effects which are of assistance in recognizing the presence of such impurities and their extent.

The detection and compositional evaluation of anhydrous carbonate minerals is of considerable economic value and importance to, for instance, the ceramic, cement, plaster, glass, petroleum, agricultural, smelting, coal utilization industries and is of considerable importance in the potential use of oil shales as a source of hydrocarbon fuels.

In these industries the presence of particular carbonates and their impurities can be either sought after or cause deleterious effects. For example, the iron contents of carbonates may be indicative of associated heavy metal deposits and can give information on depositional and diagenetic environments. On the other hand, siderite specifically represents not only an ore of iron, a vein mineral with economic mineral deposits, but gives strong coloring and physical effects in glass manufacture, and lowers the ash fusion point of coals [8] and oil shales.

The experimental situation is difficult because extremely low partial pressures of oxygen are required to maintain the reduced oxides of iron in the temperature region of interest. Furthermore, wustite (FeO) is unstable below 563° C with respect to disproportionation into iron and magnetite (Fe_3O_4) [eqn. (1)].

$$4\ Fe_2O_3 \rightarrow Fe_3O_4 + Fe \qquad (1)$$

Table 1 gives selected values derived from a Richardson—Jeffers type plot [9]. The CO_2 released from the carbonate decomposition is thermodynamically quite capable of oxidizing the wustite produced and the question pertains to the mechanism of the decomposition in an inert atmosphere. Mechanism I assumes that the decomposition product is wustite and any magnetite that appears is based upon a reaction with the atmosphere which to some ill-defined extent includes its own decomposition product [eqn. (2)].

Mechanism I $\qquad FeCO_3 \rightarrow FeO + CO_2 \qquad (2)$

TABLE 1

Approximate equilibrium partial pressures of O_2 associated with various iron oxidation equilibria

	$-\log P_{O_2}$(atm)			CO/CO_2
	400°C	500°C	600°C	
$Fe + 2/3\ O_2 \rightarrow 1/3\ Fe_3O_4$	35	29		
$FeO + 1/6\ O_2 \rightarrow 1/3\ Fe_3O_4$			25	~1
$1/3\ Fe_3O_4 + 1/12\ O_2 \rightarrow 1/2\ Fe_2O_3$	22	18	14	$\sim 10^{-6}$

Mechanism II assumes that thermodynamic equilibrium is established during the bond breaking process associated with the decomposition and that no wustite is formed [eqn. (3)].

Mechanism II $$3\ FeCO_3 \rightarrow Fe_3O_4 + CO + 2\ CO_2 \quad (3)$$

Obviously, as the speed and probability of the secondary reaction in mechanism I increases, the two mechanisms become indistinguishable. In the presence of atmospheric oxygen the reduced oxide and any CO formed would be immediately oxidized [mechanism III, eqn. (4)].

Mechanism III $$2\ FeCO_3 + \tfrac{1}{2}\ O_2 \rightarrow Fe_2O_3 + 2\ CO_2 \quad (4)$$

Typical divalent impurities of suitable size, e.g. Mg and Mn, are assumed to dissolve in either the wustite or magnetite phases while Ca is presumed too large to have significant solubility. In the case of mechanism III it is expected that enough spinel second phase (MFe_2O_4) will form to accommodate the divalent impurities and still allow for all of the iron to be trivalent. Other common impurities are anticipated to form and segregate in an extraneous calcium silicate phase because of their low solubility in the iron oxide phases.

Thermomagnetometry (TM) has proven useful in studying phase relationships in certain systems [10,11]. Since both the various spinel phases and the hematite (α-Fe_2O_3) are magnetically oriented well above room temperature, it should also be informative for the study of the decomposition of siderite. This technique is coupled with conventional thermogravimetry (TG) and mass spectrographic evolved gas analysis (EGA) in an effort to establish the sequence of oxidation of the divalent iron and to confirm the expected behavior of various major impurities in siderite.

EXPERIMENTAL PROCEDURES

The purity and source of the three samples of siderite used in this work are given in Table 2. Analyses were performed by wet chemical methods. Samples of magnesium ferrite ($MgFe_2O_4$), manganese ferrite ($MnFe_2O_4$), and an equimolar mix of the two were prepared by calcination of the appropriate coprecipitated oxalates (Alfa Inorganics) in air overnight at 1000° C. Magnetite and hematite were from Fisher Scientific and Pfizer Chemical Companies, respectively. The calcium carbonate was a sieved 20—44 μm fraction of J.T. Baker reagent grade.

A Perkin—Elmer TGS-1 thermobalance was used which had been modified to take data in a digital manner [12]. Calibration of the temperature axis was achieved using magnetic standards [13]. The temperature was also monitored by a chromel—alumel thermocouple; however, this method was judged inferior to the magnetic calibration [10]. Thermogravimetric experiments were performed using 4—12 mg samples in flowing (40 cc min^{-1}) N_2 or O_2 at a heating rate of 10° C min^{-1}. The gas stream was dried by passing it through a column of molecular sieve. Decrepitation of the mineral samples was a problem so a tared platinum mesh screen was used as a cover.

TABLE 2

Composition of siderites in mole %

	A	B	C
$FeCO_3$	95.3	85.5	81.7
$MnCO_3$	4.2	4.0	6.4
$MgCO_3$	0 4	7.6	9.5
$CaCO_3$		0.9	1.5
SiO_2		1.9	0 5
R_2O_3			0.1
H_2O	0.1	0.1	0

A Kryolitselskabet Oresund A/S, Copenhagen, Denmark.
B Roxbury, Connecticut, U.S.A.
C Broken Hill, New South Wales, Australia.

A small $SmCo_5$ permanent magnet was used to provide a field gradient (~800 gauss at the sample) for the TM experiments. Heating and flow rates were the same as those employed for TG. Sample sizes ranged from 4—16 mg.

Several modifications were made to the previously described EGA apparatus [14]. A UTI model 2054 programmable peak selector was used to program the mass spectrometer and collect the data. A Netzch model 411 controller was used to program the furnace temperature. A Fluke model 2190A digital thermometer coupled with a Spectrum model 1021 filter/amplifier (10X) was used to supply the temperature input for the programmable peak selector. The heating rate was 10°C min^{-1} and the vacuum ranged from 1×10^{-7} to about 1×10^{-4} Torr depending upon the extent of the decomposition. Again decrepitation was a problem and a small (1—2 mg) plug of quartz wool was used to prevent loss of material from the alumina crucible.

X-Ray diffraction patterns of selected powdered samples were obtained using an automated Diano XRD-8000 diffractometer and $CuK_{\alpha 1}$ radiations.

RESULTS AND DISCUSSION

Figures 1—3 show the TG results for the thermal decomposition of the three siderite samples in N_2 and O_2. Table 3 summarizes the weight losses observed and compares them with calculated values based upon the chemical analyses in Table 2 and the three mechanisms described in the Introduction. Compositions of the end products based upon these three decomposition schemes are listed in Table 4. Inspection of Figs. 1—3 indicates that the decomposition temperature in oxygen is higher than in nitrogen and that the decomposition temperature increases with decreasing purity.

The values in Table 3 for the purest sample, A, agree quite well with decomposition directly to magnetite followed by a slow oxidation in the nitrogen stream (1—10 ppm O_2) to finally yield hematite at the highest tem-

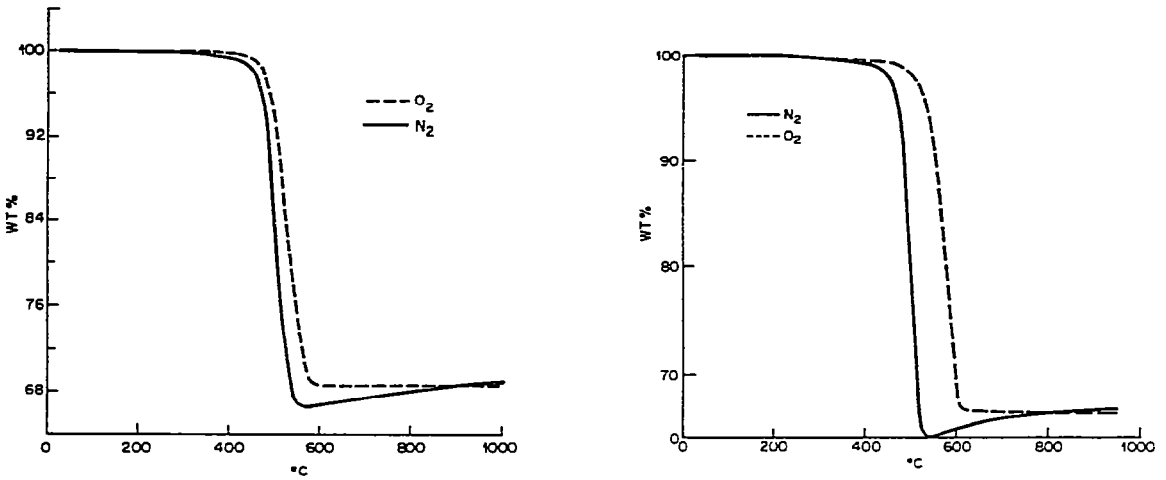

Fig. 1. TG of siderite A. (a) 11.16 mg in N_2; (b) 5.23 mg in O_2.

Fig. 2 TG of siderite A. (a) 6.29 mg in N_2, (b) 5.02 mg in O_2.

perature. The decomposition in oxygen yields hematite directly, at least within the time scale of this experiment.

The weight losses for samples B and C, however, do not conform so well to that sequence. There is the same slow pick up of about 2 wt.% between the minimum value and the end value in nitrogen. However, all the values seem low by about 1%. Even the weight loss in oxygen for sample B seems to be low by a similar amount. There is the problem associated with obtaining a truly representative sample when using only 5—6 mg samples of a mineral and this may be partially responsible. Another possibility is that the minerals had absorbed contaminants from the atmosphere, e.g., water, since their analysis. However, an early ($\leqslant$200°C) 1 wt.% loss is not evident in Figs. 2 or 3 which tends to exclude that possibility. Yet another possibility is that the product is reduced beyond magnetite and that the spinel phase stabilizes

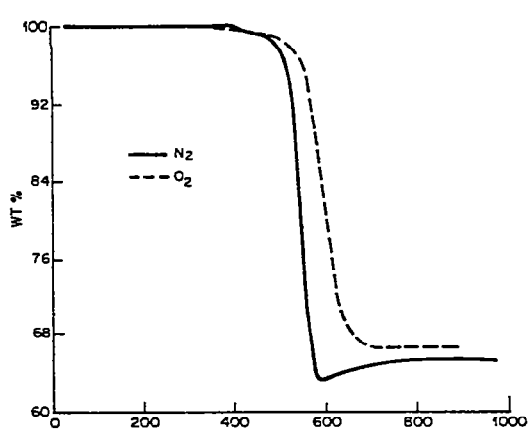

Fig. 3. TG of siderite C. (a) 6.07 mg in N_2; (b) 6.14 mg in O_2.

TABLE 3

Calculated and observed weight losses for several siderites (values are wt.% remaining)

Siderite	Calculated			Observed		
	I	II	III	N_2(Minimum)	N_2(end)	O_2(end)
A	62.5	66 9	69.0	66.8	69.0	68.7
B	61.5	65.6	67.6	64.4	66.6	66.5
C	61.0	64 9	66 9	63.3	65.3	66.5

some divalent iron from subsequent reoxidation in the nitrogen stream and even in oxygen. The latter would mean that the compositions in column III of Table 3 should include more iron in the spinel phase and less hematite.

The EGA experiments describe the decomposition in vacuum and hopefully provide evidence to help decide between mechanisms I and II. The clues to help distinguish this should be: (a) the relative amounts of carbon monoxide and dioxide; (b) the sequence in temperature and time of their evolution; (c) the presence or absence of any separate evolution of oxygen; and (d) the X-ray diffraction pattern of the residue after the decomposition in vacuum. In order to provide a frame of reference for the first three points, EGA experiments were performed on calcium carbonate and hematite. Calcium carbonate will provide an example where CO_2 is unequivocally the only product gas and hence the cracking pattern of carbon dioxide can be established on this instrument under similar conditions of pressure, temperature, geometry, and rate of evolution. Figure 4 shows the results of such an experiment. The mass 44 (CO_2^+) and mass 28 (CO^+, N_2^+) peaks are in complete registration with respect to temperature and time. The cracking pattern for carbon dioxide under these experimental conditions is 44(100), 28(17), 16(13), 12(8) and 22(0.3).

Figure 5 shows the evolution of oxygen as hematite is heated in a vacuum of about 1×10^{-7}. Hematite begins to form magnetite at about 850° C and the magnetite subsequently begins to form wustite around 1260° C. Checking these temperatures on a Richardson—Jeffers type plot [9], they suggest a P_{O_2} of about 5×10^{-8} which seems reasonable for the detection threshold at the sensitivity setting used for the mass spectrometer. The experiment demonstrates that hematite is relatively stable below approximately 800° C and magnetite below about 1200° C in the vacuum system of the EGA. Thus the appearance of wustite or magnetite in the decomposition products of siderite below 800° C in the EGA is not due to reduction of magnetite or hematite by the vacuum.

The EGA results for siderites A, B, and C are presented in Figs. 6—8, respectively. There was only a low background for mass 32 in all cases, i.e., no evolution of oxygen. The mass 28 peaks ranged from 22—24% of the mass 44 peaks. This indicates that about one-third of the mass 28 peak was due to carbon monoxide formation and the balance to the cracking pattern of the carbon dioxide. In addition, the two peaks are clearly not aligned for

TABLE 4

Calculated compositions of the decomposition products of several siderites and their estimated Curie temperatures for the spinel phases

Siderite	Decomposition scheme		
	I	II	III
A	$Fe_{0.954}Mn_{0.042}Mg_{0.004}O$	$(Mn_{0.126}Mg_{0.012}Fe_{0.862})Fe_2O_4$ (547°C)	0.90 Fe_2O_3 0.10 $(Mn_{0.91}Mg_{0.09})Fe_2O_4$ (313°C)
B	$Fe_{0.881}Mn_{0.041}Mg_{0.078}O$	$(Mn_{0.120}Mg_{0.236}Fe_{0.644})Fe_2O_4$ (517°C)	0.73 Fe_2O_3 0.27 $(Mn_{0.35}Mg_{0.65})Fe_2O_4$ (391°C)
C	$Fe_{0.838}Mn_{0.065}Mg_{0.097}O$	$(Mn_{0.191}Mg_{0.285}Fe_{0.524})Fe_2O_4$ (489°C)	0.61 Fe_2O_3 0.39 $(Mn_{0.40}Mg_{0.60})Fe_2O_4$ (384°C)

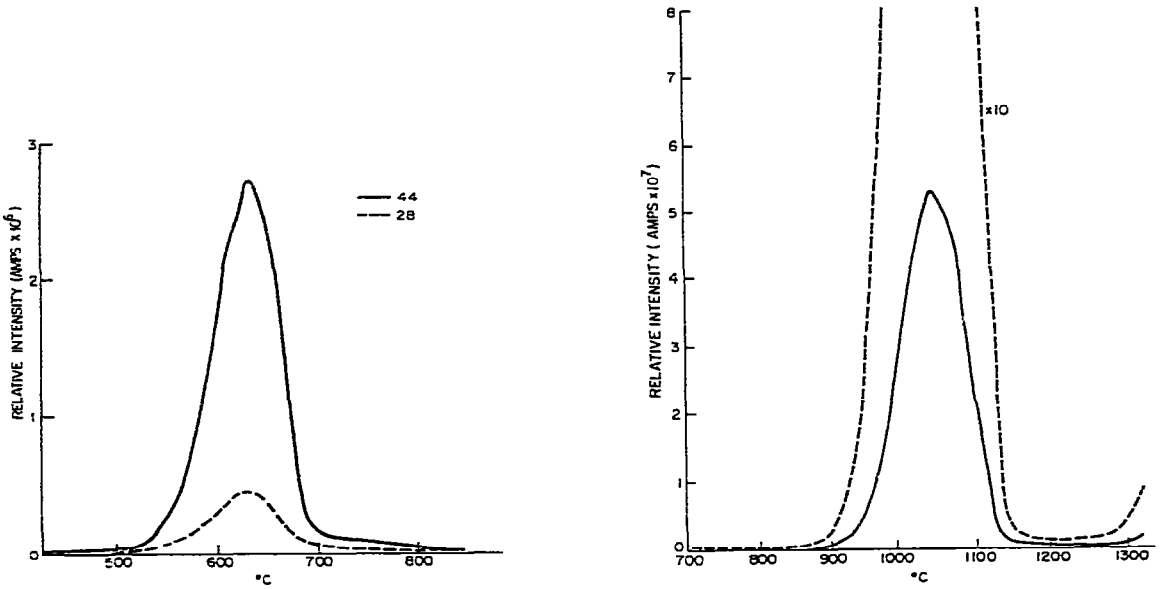

Fig. 4. EGA curves for $CaCO_3$, 6.80 mg. (a) Mass 44; (b) mass 28.

Fig. 5. EGA curves for α-Fe_2O_3, 12 1 mg (a) Mass 32; (b) mass 32, 10X sensitivity.

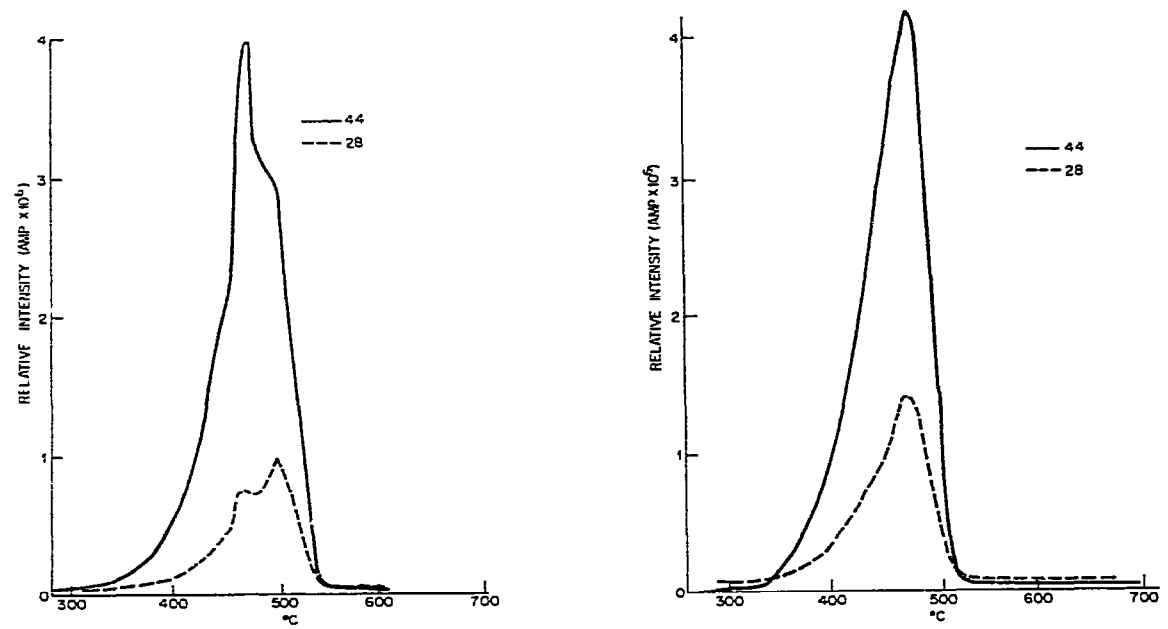

Fig. 6. EGA curves for siderite A, 10.3 mg. (a) Mass 44; (b) mass 28.

Fig. 7. EGA curves for siderite B, 9.5 mg. (a) Mass 44; (b) mass 28.

the case of the high purity siderite A in Fig. 6. These facts establish that some carbon monoxide is formed and that in at least one case the detection of the carbon monoxide seems to lag that of carbon dioxide.

Larger quantities, about 50 mg, of the siderites were fired in the same vacuum system to 600°C and then cooled as rapidly as the furnace will naturally cool in the vacuum. X-Ray diffraction analysis of the residues indicate predominantly wustite with some spinel. The relative quantity of spinel varied A > C > B. The presence of wustite under these conditions indicates that the reaction proceeds via mechanism I. The presence of the spinel and carbon monoxide is attributed to a very rapid reaction of a portion of the carbon dioxide evolved according to eqn. (5)

$$3\ FeO + CO_2 \rightarrow Fe_3O_4 + CO \qquad (5)$$

Also, it must be recalled that wustite is unstable below 563°C and that at least some of the magnetite can result from the disproportionation [eqn. (1)]. The much smaller amount of iron formed may be microcrystalline or amorphous so that it is not readily detected by X-ray diffraction. Yet a third possibility can be oxidation by the air in the time between the removal of the sample from the vacuum and its subsequent X-ray diffraction analysis. Regardless of the extent of these latter possibilities, some magnetite must result from oxidation by the carbon dioxide produced in order to explain the detection of significant amounts of carbon monoxide. The extent and nature of the impurities may also influence this reaction through stabilization of a spinel phase. If this reaction is sufficiently fast to occur in vacuum where the gaseous products are removed rapidly, then they surely have an

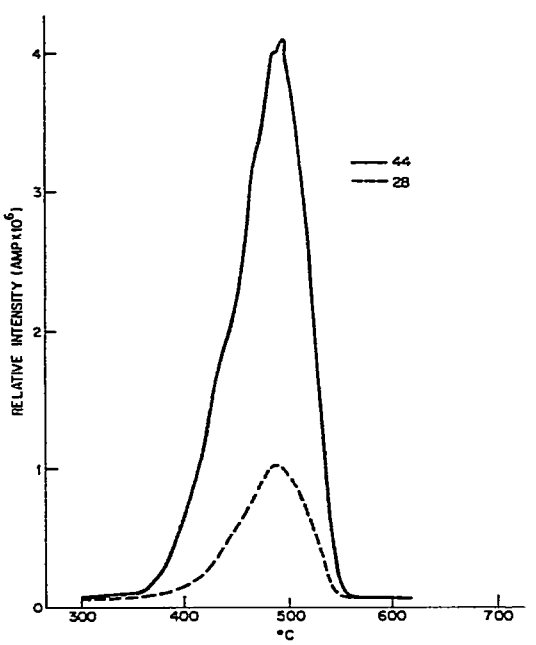

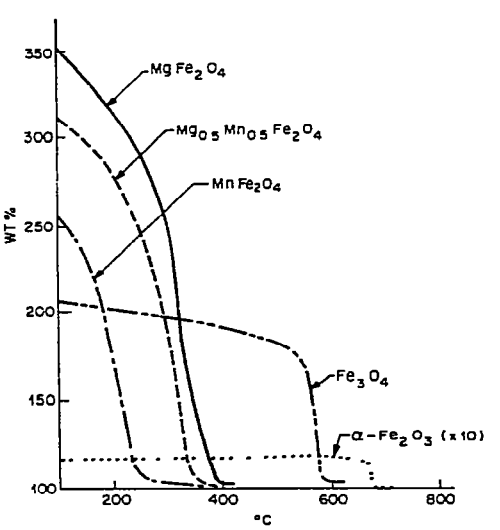

Fig. 8. EGA curves for siderite C, 11.8 mg. (a) Mass 44; (b) mass 28.

Fig. 9. TM curves for various oxides of iron.

opportunity to occur during the conventional TG experiments at atmospheric pressure where there would be locally a greatly increased partial pressure of self-evolved carbon dioxide.

All the spinel phases formed during the decomposition of the siderite are ferrimagnetic with Curie temperatures, T_C, above room temperature. Although hematite is antiferromagnetic, there is a weak parasitic ferromagnetic component which arises from the canted spins [15]. This can be detected at high sensitivity. Figure 9 shows TM curves for several oxides which are relevant to this investigation. Reported values of T_C are given in Table 5 [16]. Excellent agreement exists between the reported values and those deduced from Fig. 9 for the simple oxides, hematite and magnetite. The substituted spinels, however, are much more subject to variance due to slight differences in cation ratios, oxygen stoichiometry, site preference, and particle size. The first depends upon the synthesis and the latter three are established by the thermal history. The somewhat lower T_Cs observed may be due to an iron deficiency or partial oxidation. The hypothetical values of T_C given in Table 4 are calculated using the reported values for the pure compounds in Table 5 and the assumption of a linear dependence of T_C upon composition for the solid solution.

A series of TM curves for siderite A is shown in Figs. 10—12. The starting weight of the sample in the absence of a magnetic field is taken as 100 wt.%. All three siderites tended to gain about 0.5—1.2 wt.% at room temperature when the field gradient was imposed.

The decomposition in nitrogen (Fig. 10) begins around 400° C as it did in the absence of a magnetic field. As the wustite originally formed becomes oxidized by the carbon dioxide, magnetite is formed. These magnetite nuclei grow until they are of sufficient size and crystalline perfection to magnetically order. This gives rise to an apparent weight gain in the magnetic field gradient because the sample is still below the T_C for the spinel phase. As the T_C of this phase is exceeded, the weight quickly adjusts to the weight loss curve in the absence of a magnetic field. The T_C of the spinel phase in Fig. 10 seems to be in good agreement with that predicted for the single phase spinel in Table 4 (~550° C).

In oxygen, however, the wustite is so rapidly oxidized to hematite that the strongly magnetic spinel phase never has a chance to form, and the only

TABLE 5

Reported Curie Temperature, T_C, for selected compounds

Compound	T_C(°C)
α-Fe_2O_3	675
γ-Fe_2O_3	~585
Fe_3O_4	585
$MgFe_2O_4$	440
$MnFe_2O_4$	300
Mn_3O_4	—230

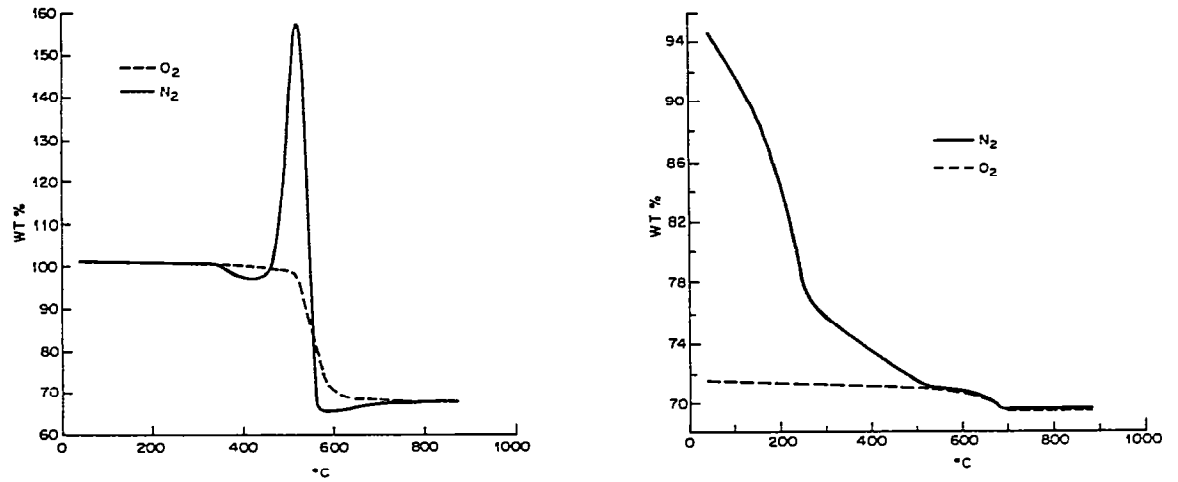

Fig. 10. TM curves for siderite A. (a) 8.588 mg in N_2; (b) 8.429 mg in O_2.

Fig 11. TM curves for the residues in Fig 10. (a) N_2 residue in N_2, (b) O_2 residue in O_2.

magnetically induced perturbation that is evident is the slight drop at about 675° C indicative of the parasitic ferromagnetism in hematite.

The decomposed samples were reheated in the same atmosphere without disturbing the balance/magnet arrangement. These TM curves are presented in Fig. 11. The slow oxidation that takes place at higher temperatures has markedly changed the TM curve for the sample run in nitrogen. The 100% value represents the original starting weight of the siderite in the absence of the magnetic field, i.e., it is the same scale as in Fig. 10. The sample now appears to be multiphase with considerable hematite indicated by the apparent weight loss near 675° C. The spinel phase does not appear homogeneous, with a break near 300° C indicating manganese ferrite, and another around 500° C which implies a mixed ferrite including some divalent iron. In oxygen only hematite is evident, implying that the major impurity, manganese, has probably been oxidized to the trivalent state and incorporated into the hematite phase as has been observed elsewhere [17]. The small amount of magnesium is not detected magnetically, suggesting that there is no spinel present and that the magnesium has been rejected to form a small amount of a second phase of its own.

The material calcined in vacuum had been shown to be wustite with some spinel by X-ray diffraction analysis. Figure 12 shows the TM curve for the material both heated (curve 1) and reheated in nitrogen again without disturbing the balance/magnet relation (curve 2). The starting weight of the calcine in the absence of a magnetic field represents the 100% value. The initial heating of the wustite, curve 1, shows that there is a significant amount of magnetic spinel phase present initially and that the amount increases as the wustite is slowly oxidized by the oxygen impurity in the nitrogen stream. This is a slower process than that indicated in Fig. 10 because carbon dioxide is absent. There is a sharp apparent weight loss at the T_C of the spinel phase.

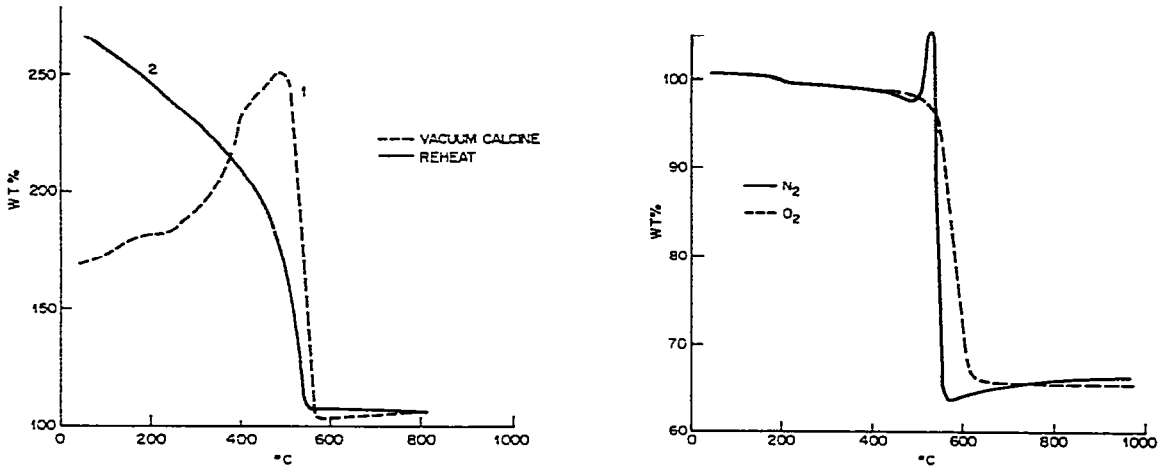

Fig 12. TM curves in N_2 for siderite A after calcination in vacuum. (1) 4.943 mg — 1st heating; (2) reheating.

Fig. 13. TM curves for siderite B. (a) 8.073 mg in N_2; (b) 4.193 mg in O_2.

Again the T_C agrees well with that predicted for the single phase spinel in Table 4. Upon reheating (curve 2) there is no wustite phase to be oxidized and only the spinel phase with some hematite is obvious. The hematite could be inferred from the weight gain present at higher temperatures in the initial heating (curve 1). It would also have been predicted from Figs. 10 and 11.

The TM analyses for the other siderites reflect the same general thinking but differences arise due to the increased impurity contents, magnesium in particular. The analogous curves for siderite B are presented in Figs. 13—15. Because of the increased impurity content, T_C of the spinel phase is lower. Consequently, the apparent weight gain in nitrogen is less in Fig. 13 than for

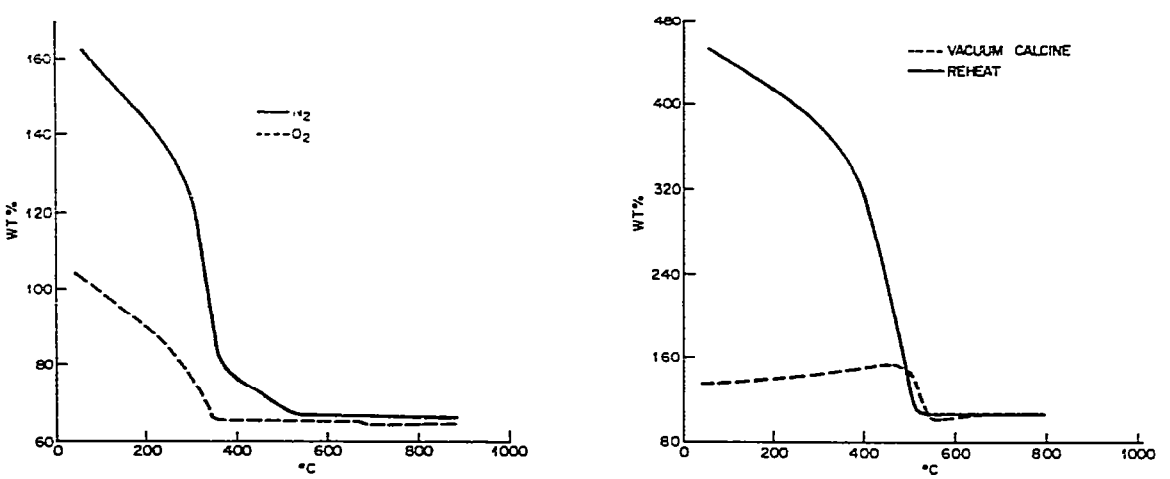

Fig. 14. TM curves for the residues in Fig. 13 (a) N_2 residue in N_2; (b) O_2 residue in O_2.

Fig. 15. TM curves in N_2 for siderite B after calcination in vacuum. (a) 8.073 mg — 1st heating; (b) reheating.

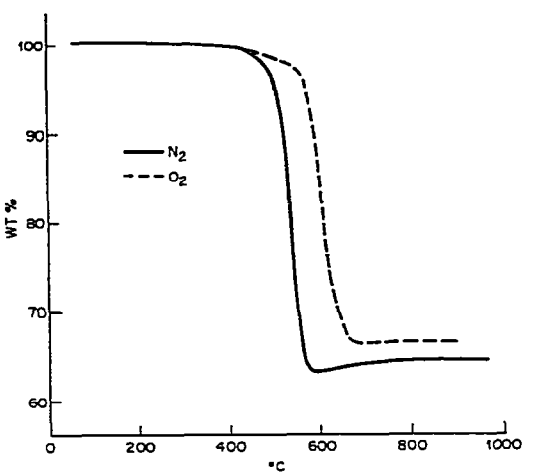

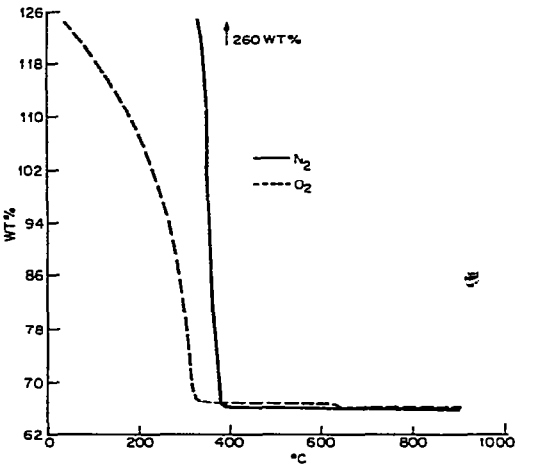

Fig. 16 TM curves for siderite C (a) 16.456 mg in N_2; (b) 8.543 mg in O_2.

Fig 17. TM curves for the residues of Fig. 16. (a) N_2 residue in N_2; (b) O_2 residue in O_2.

the previous material. In Fig. 14 the TM curves of residues also show displacement towards lower T_C values consistent with the trend indicated by the speculated values given in Table 4. The presence of hematite is also obvious from the apparent weight change around 675°C. This is greater in oxygen than in nitrogen, as would be expected.

The TM curves for the material calcined in vacuum show less apparent weight gain during the initial heating. Upon reheating, the material appears more homogeneous and very similar to that observed earlier for siderite A.

The T_C for the spinel formed by the decomposition of siderite C has dropped so low, due to the highest impurity content, that there is no apparent weight gain in the TM curve in N_2 (see Fig. 16). Upon reheating (Fig.

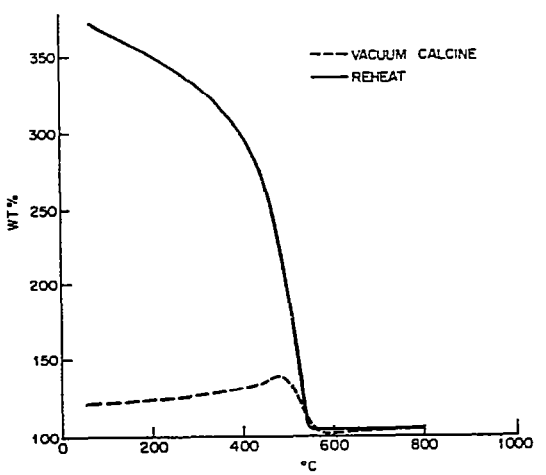

Fig. 18. TM curves for siderite C after calcination in vacuum. (a) 3.270 mg — 1st heating; (b) reheating.

17), the T_C is shown to be <400°C and hence one would not expect to see the magnetic effect during the initial decomposition which starts above 400°C. Again, the hematite is much more evident in the experiments performed in oxygen.

Finally, the TM curves for siderite C calcined in vacuum (Fig. 18) are very similar to those for siderite B. The values of T_C are shifted towards lower temperatures, as would be expected. In every case the T_C of the spinel phase for materials calcined in vacuum is higher than that calcined in nitrogen or oxygen. This indicates that for any given purity the amounts of divalent iron and total iron in the spinel, and hence the percentage of the spinel phase, increase with increasing reducing power of the atmosphere during the formation of the spinel.

CONCLUSIONS

The thermal decomposition of siderite occurs via the production of wustite and carbon dioxide. The partial pressure of oxygen necessary to preserve this wustite is exceedingly low and hence immediate interaction with the furnace atmosphere occurs. Some interaction with carbon dioxide produced is inevitable, as shown by the significant amount of the reaction occurring in vacuum. In a flowing inert gas stream, it appears that magnetite will result from this interaction. In air or oxygen the oxidation is so rapid that only hematite is detected. The nature and extent of impurities, e.g., magnesium and manganese, will have a significant effect on the phases formed during the decomposition.

Thermomagnetometry is a useful technique to show the presence of intermediate magnetic phases during the decomposition. If the Curie temperature of the resulting spinel phase is depressed below the decomposition temperature of the siderite then intermediates cannot be detected magnetically. The end product, however, can be evaluated by this technique to aid in determining the distribution of the impurities. Furthermore, the degree of purity of naturally occurring siderites is indicated as the T_C of the spinel formed from their thermal decomposition falls with increasing impurity contents.

ACKNOWLEDGEMENT

The authors are grateful to Mr. F. Schrey for performing the X-ray diffraction measurements.

REFERENCES

1 S.St.J. Warne, Bull. Soc. Fr. Mineral. Cristallogr., 84 (1961) 234.
2 T.L. Webb and J.E. Krüger, in R.C. Mackenzie (Ed), Differential Thermal Analysis, Vol. I, Academic Press, London, 1970, Ch. 10, pp. 303—341.
3 K. Smykatz-Kloss, Differential Thermal Analysis Applications and Results in Mineralogy, Springer-Verlag, Berlin, 1974, p. 185

4 S.St.J. Warne, Chem. Erde, 35 (1976) 251.
5 Z. Kubas and M. Szalkowicz, in Thermal Analysis, Vol. 2, Proc 3rd ICTA Conf, Davos, Switzerland, 1971, pp. 447—461.
6 W.A. Deer, R.A. Howie and J. Zussman, Rock Forming Minerals, Vol. 5, Longmans, Green and Co. Ltd, 1964, p. 371.
7 E.S. Dana and W.F. Ford, A Textbook of Mineralogy, John Wiley and Sons, London, 1958, 4th edn., p. 851.
8 S.St.J. Warne, Proc. 5th Int. Confed Therm. Anal. Conf. (Kyoto, Japan), 1977, p.460.
9 R.A. Swalin, Thermodynamics of Solids, J. Wiley, New York, 1967, p. 84.
10 P.K. Gallagher, E. Coleman, S. Jin and R.C. Sherwood, Thermochim. Acta, 37 (1980) 291.
11 R. Moskalewicz, Thermochim. Acta, 28 (1979) 229.
12 P.K. Gallagher and D.W. Johnson, Jr., Thermochim Acta, 4 (1972) 283
13 P.K. Gallagher and F. Schrey, Thermochim. Acta, 1 (1970) 465.
14 P.K. Gallagher, Thermochim. Acta, 1 (1970) 465.
15 I. Dzyaloshinsky, J. Phys. Chem. Solids, 22 (1958) 617
16 J.B. Goodenough, Magnetism and the Chemical Bond, J. Wiley, New York, 1963, p 148.
17 D.W. Johnson, P.K. Gallagher, M.F. Yan and H. Schreiber, J. Solid State Chem., 30 (1979) 299.